Individually addressable multi-nanopores for single-molecule targeted operations

Paolo Cadinu[1], Minkyung Kang[1], Binoy Paulose Nadappuram[1], Aleksandar P. Ivanov[1], Joshua B. Edel[1]

Department of Chemistry, Imperial College London, Molecular Science Research Hub, White City Campus, 80 Wood Lane, W12 0BZ, UK.

† Corresponding authors: alex.ivanov@imperial.ac.uk, joshua.edel@imperial.ac.uk

Abstract

The fine-tuning of molecular transport is a ubiquitous problem of single-molecule methods. The latter is evident even in powerful single-molecule methods such as nanopore sensing, where the quest for resolving more detailed biomolecular features is often limited by insufficient control of the dynamics of individual molecules within the detection volume of the nanopore. In this work, we introduce and characterize a reconfigurable multi-nanopore architecture that enables additional channels to manipulate the dynamics of DNA molecules in a nanopore. We show that the fabrication process of this device, consisting of four adjacent, individually addressable nanopores located at the tip of a quartz nanopipette, is fast and highly reproducible. By individually tuning the electric field across each nanopore, these devices can operate in several unique cooperative detection modes that allow moving, sensing, and trapping DNA molecules with high efficiency and increased temporal resolution.

Keywords:

single-molecule sensing, multi nanopore architecture, biophysics, Nanopore sensing

Improving the ability to detect and analyze one molecule at a time is at the forefront of today's research in medicine, biophysics, and analytical sciences. The constant demand for enhancing and developing sensitive tools derives from the recognized importance of capturing as much information as possible from single molecules. For example, such an approach can help to unravel complex biochemical pathways[1], detect aberrant species associated with pathologies, and, more generally, study the heterogeneity of a population otherwise hidden in the noise of an ensemble-averaged measurement. Recently, nanopore sensing has arisen as one of the most promising technologies capable of meeting this growing demand for label-free single-molecule detection[2,3]. However, to accurately identify a biomolecule and thus determine its molecular properties such as geometry, size, conformation, charge, abundance, it is of utmost importance to fine-tune transport across the sensing region. Understanding how to improve control and optimize molecular transport at the single-molecule level has been a priority within the nanopore community[4]. Historically, challenges associated with spatial and temporal resolution derived from poor transport control, has been tackled with i) chemical modification[5,6] ii) changing materials and pore geometry[7–9] iii) electrochemically[10–12] iv) using entropic and plasmonic traps[13–15] v) adding functionality incorporating hybrid field-effect transistor nanopore systems[16–19]. However, these solutions come at the expense of increased fabrication complexity and scalability.

Recently, double nanopore platforms[20–26] has been gaining momentum in part due to their capability in improving the detection of a broad range of biomolecules by actively manipulating their transport at the nanoscale. Rather than tuning the physicochemical parameters of the nanopore, multi-nanopore structures are more flexible and leverage cooperative sensing modalities between the different pores. These additional degrees of freedom arise from the possibility of independently applying a bias to each pore, which in turn allows for fine-tuning of the electric field near the aperture, and consequently fine-tuning the pore-to-molecule interaction. This enables the possibility of carrying out several operations on a molecule of interest, including trapping and stretching as well as performing simultaneous readout from multiple nanopores. To date, different architectures have been proposed, including planar[27] and stacked[28] arrangements on Si-based membranes, and micro-nano fluidic systems coupled with double nanopores.[20,29] However, double-barrel nanopipettes have recently emerged as a simple, yet robust solution.[24,30,31] Aside from ease of fabrication, and cost-effectiveness, multi-barrelled nanopipettes offer unique modes of sensing which are not typically available when using membrane-based solid-state or biological platforms.

Here we present a programmable multi-nanopore architecture consisting of four adjacent independently controllable nanopore channels, each being separated by a nanometric gap of approximately 20 ± 4 nm. We show that by individually addressing each nanopore the device can be reconfigured in real-time allowing for i) three and four-barrel operation where molecules are stretched trapped and detected with higher signal-to-noise ratio (SNR) ii) higher throughput achieved by simultaneously using multiple nanopores iii) increased trapping efficiency and iv) single-molecule enhanced sensing where a targeted molecule is read multiple times via dynamical manipulation across the pores.

Similar to single and double-barrel nanopore architectures using pipettes, quad-barrel nanopores were fabricated by laser-assisted pulling [32–34] of quad-barrel quartz capillary resulting in nanopipette tip terminating with four individual nanopores as shown in Figure 1. The cross-section of the tip was a rounded square, whereas each nanopore was quadrant-shaped (Figure 1b). The overall diameter of the apex was 149 ± 23 nm, whereas the diameter of a single nanopore was, on average, 40 ± 12 nm as measured by scanning electron microscope (SEM, n = 12). Nanopores were separated from each other with a 20 ± 4 nm thick quartz septum, and the outer wall thickness was 22 ± 4 nm, respectively (Figure 1c, SI Figure 1, SI Table 1). Notably, the septum spanned from the end of the tip to the back aperture of the nanopipette, ensuring electrical insulation between the barrels. In a standard experiment, much

like with nanopipettes with single nanopores, each barrel was filled with an electrolyte solution, and an independent working electrode was connected to one of the four patch-clamp terminals of the amplifier (SI Figure 2-3). An electrode placed in the bath served as a common/reference electrode.

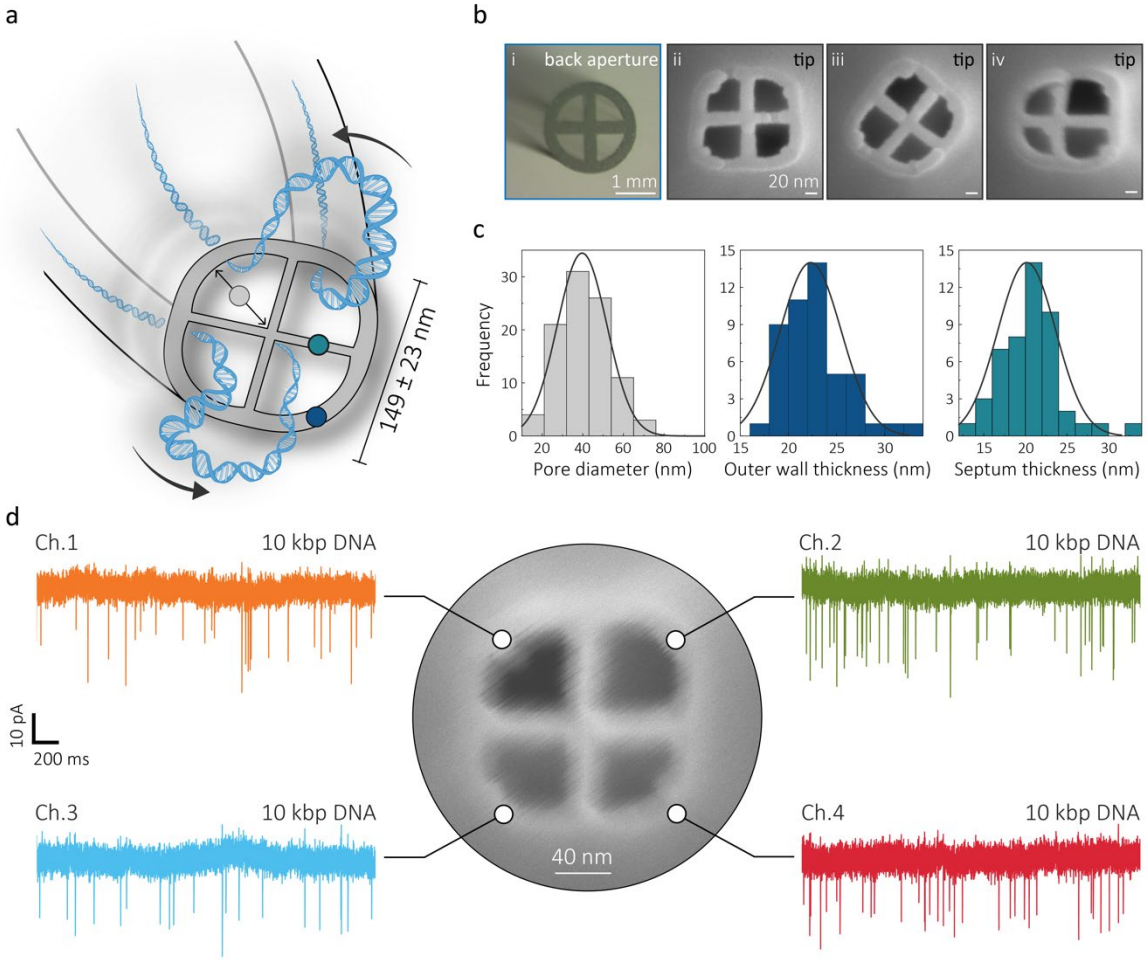

Figure 1. Experimental setup and characterization of a quad-channel nanopore. (a) Schematic representation showing DNA molecules translocating across a quad nanopore system. In all experiments, the ground electrode was placed in the bath whereas each of the 4 barrels, were provided with one independently addressable working electrode. DNA molecules were inserted either in the bath or in one of the barrels, and, depending on the experiment, they were either threaded across a single pore, clamped between two pores or transported, and thus detected in rapid succession from one pore to the other. (b) Bright-field and SEM images of the quad barrel nanopipettes showing the tip and the back aperture respectively (c) The pore radius was measured to be 40 ± 12 nm, cone angle of ~0.12 radians, inner septum and outer wall of 20 ± 4 and 22 ± 4 respectively (n = 12 devices). (d) Ionic current traces measured in 100 mM KCl buffered in TE at pH 8 showing 10 kbp DNA molecules detected while translocating from inside the barrels to the bath. Errors denote one standard deviation.

Potential leakage between barrels (solution leakage and electrical crosstalk) was characterized by varying the potential applied to one channel at a time since it would limit the ability to modulate the bias in each channel individually. The leakage of the ionic current in the inactive channels was calculated to be as low as 1% (SI Figure 4) and well within noise levels. The crosstalk observed likely originates from parasitic capacitance, which, as a result of sudden changes in bias applied, generated a spike-like type of response (high in amplitude, short in time), in the ionic current recordings. The power spectral density of individual channels showed a similar profile when compared to a single or double barrel device, and the activation of all channels does not influence the noise levels (SI Figure 5). Current-voltage (IVs) curves using 100 mM KCl exhibited typical ionic current rectification[35,36]. The average open pore conductance was measured to be 10.2 ± 2.3 nS, however, within the same nanopipette, conductance variability dropped significantly (e.g., 10.2 ± 0.5 nS SI Figure 6) reflecting a smaller pore-

to-pore variation observed in the SEM micrographs. As part of the initial characterization, we showed that these devices could be used for detecting individual DNA molecules.

To characterize the translocation of bioanalytes in these devices, a negative voltage was applied in one channel at a time. The barrels were loaded with 10 kbp DNA, which was electrophoretically threaded into the bath giving rise to current enhancement (Figure 1d). The shape of the translocation, as well as peak amplitude and duration, were comparable to the other three pores of the same pipette (Figure 2). For instance, at 500 mV the peak current was 20.7 ± 4.1 pA, 21.6 ± 4.2 pA, 20.9 ± 3.7 pA and 20.1 ± 3.7 and dwell times was 0.75 ± 0.21 ms, 0.67 ± 0.19 ms, 0.7 ± 0.19 ms and 0.62 ± 0.18 for nanopore 1,2,3 and 4 respectively (Figure 2a,b). As expected, by increasing the voltage, peak current, and dwell time, as well as the SNR and capture rate, followed a similar trend across all nanopores (Figure 2c,-f). No difference was observed in the current shape and dwell time of the translocation events across different pores, and the observed signals were consistent with what was previously reported for single and double barrel nanopipettes.[30,37]

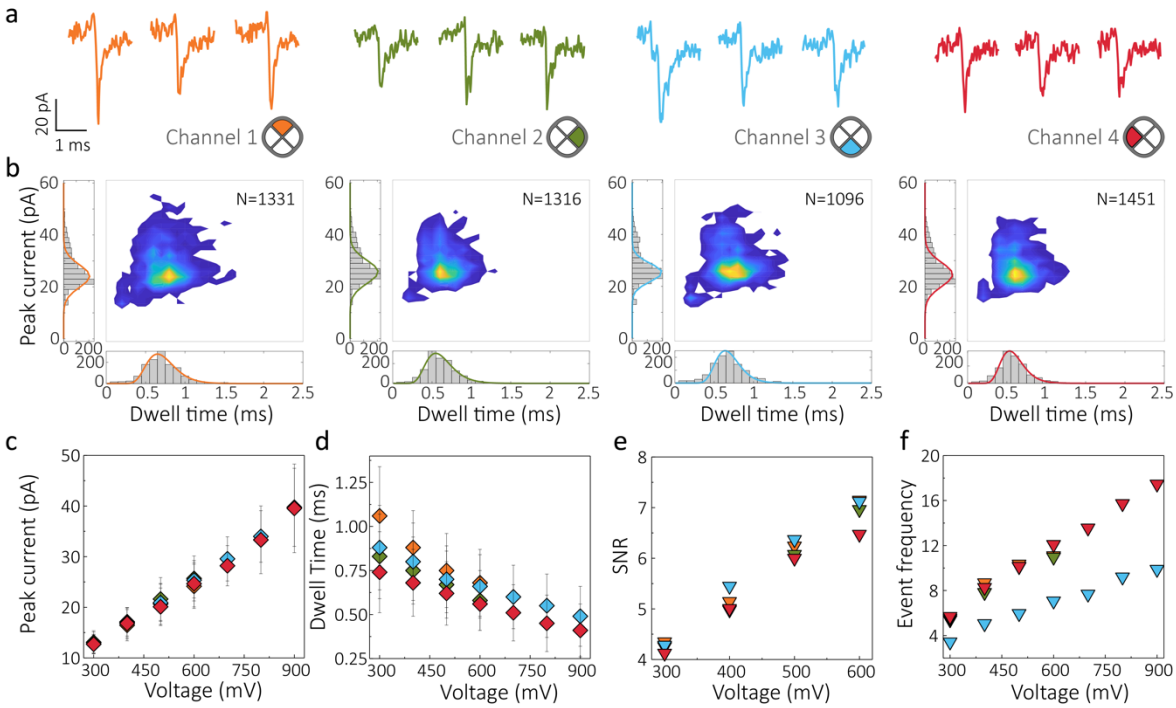

Figure 2. Single-Molecule Characterization through each barrel. (a) Representative translocation events of 10 kbp DNA molecules threaded from the pipette to the bath. In all panels, DNA was inserted in each barrel at a concentration of 400 pM in 100 mM KCl buffered in TE and a negative voltage bias with respect to the reference electrode placed in the bath was applied one barrel at a time. (b) Surface plots and relative peak current and dwell time histograms show a similar event distribution for the 4 nanopores. Voltage dependence of (c) peak current, (d) dwell time, (e) SNR and (f) capture rate of each individual nanopore channel. At higher voltages, the DNA velocity is increased, giving rise to translocation events but with higher peak amplitude and SNR. The capture shows a linear trend, in line with what it is expected for single pores. Error bars denote one standard deviation.

Harnessing four nanopores in parallel is a promising way of accomplishing high-throughput multiplexed detection of different analytes on the same platform; however, this is only one of the possible applications. We explored several sensing configurations using two to four nanopores simultaneously to controllably maneuver a molecule in the nanoscale gaps that separate these nanopores. The experiments were carried out at high salt concentration, 1 M or 2 M LiCl for the following reasons: i) reduce the electric double layer of negatively charged quartz nanopipettes, and thus electroosmotic flow, enabling DNA molecules to be ejected and recaptured ii) maximize the SNR and more importantly conserving the electrical signature shape in both direction of detection (molecule going form in to out

the pore and vice-versa). 1 M KCl has been also shown to work in this type of device however, the shape of the detected molecule is not conserved in opposite directions (neither the SNR!). iii) reducing the velocity of the threading velocity and thus increasing the spatio-temporal resolution. An example is shown in Figure 3a, where a 3-channel configuration is used to first eject a molecule from the delivery channel (negative bias with respect to the bath) and then stretched/ stalled for an extended time across the two other channels followed by recapturing the molecule (positive bias). This new configuration combines and integrates the advantages of two modus operandi, transfer, and competition mode, previously demonstrated for double-barrel nanopore devices[21]. Briefly, while holding barrels at opposite polarity with respect to the grounded bath, transfer mode enables DNA molecules to be transferred from one pore to another with near 100% efficiency. Whereas in competition mode, DNA molecules from the bath are electrophoretically attracted, threaded, and trapped across the two nanopores, which are held at a positive potential.

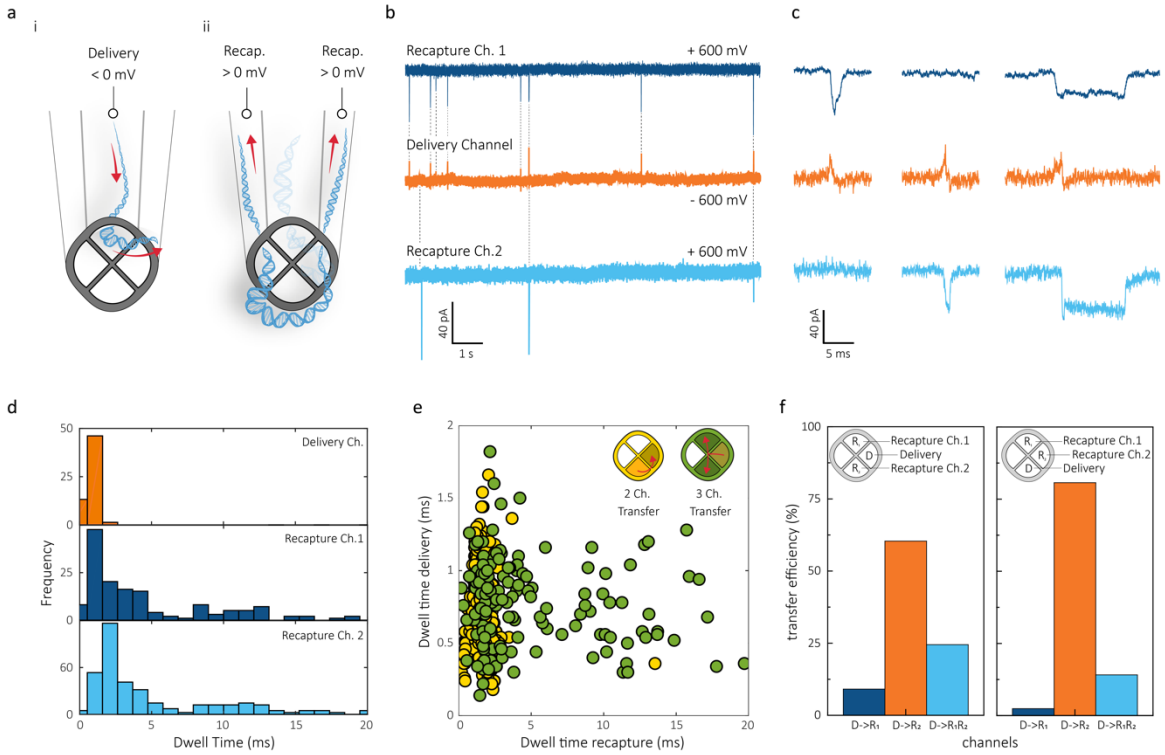

Figure 3. Schematic of quad barrel device operating under static voltage conditions. (a) Device operating in *docking + transfer* mode: one delivery channel is held at negative potential and two recapture channels are held at a positive potential. DNA molecules are ejected from the delivery channel (i) and either transferred to one of the recapture channels or, given the competing forces exerted on the DNA, eventually trapped across the recapture nanopores (ii). Ionic current traces (b) of the 3 detection channels acquired for 40 pM 20 kbp DNA molecules in 1 M LiCl. (c) Single events showing a DNA molecule ejected from the delivery channel and being transferred to one of the two recapture pores (i, ii) or being threaded at about the same time into the transfer pores as shown by the concurrent ionic current blockades peaks. Eventually, the molecule slips out of the channel exerting the weakest force ending the prolonged current blockade of its recording. (d) Dwell time histograms and (e) scatter plot showing the extended translocation time when the DNA molecule happened to be trapped across 2 recapture pores, as opposed to the single transfer where the molecule is rapidly transported from the delivery to on the recapture channels. The efficiency of these two mechanisms depends on the device bias configuration: when the delivery channel is equally distant from the recapture channels about 25% of all the molecules ejected from the delivery channel ended up experiencing a thug of war (i). This percentage drops to less than 15% when the device is biased with asymmetrically where the delivery channel is closer to one of the recapture channels. Scale bars: b) 40 pA, 1 s and c) 40 pA, 5 ms.

In the quad-barrel device, the combination of transfer and competition modes resulted in coincident events being picked up in three channels. By analyzing the shape of individual translocations, it is possible to estimate the route that the DNA molecule has followed. As an example, we show that 20 kbp DNA molecule was ejected from the delivery channel and subsequently stalled across the recapture

channels for a prolonged amount of time, as illustrated in the ionic current recordings in Figure 3b,c. Eventually, the DNA molecule escapes this trap and slips out from the nanopore that exerted the weakest force. This extended trapping time in the sensing area was measured to be at least an order magnitude longer (dwell times up to 20 ms) than the one measured either in transfer configuration or in conventional configuration (about 1 ms) where molecules are threaded from the nanopipette to the bath (Figure 3d,e). This detection by transfer and trapping mechanism offers several advantages, including a reduction in the bandwidth required and increases in the SNR.

The recapture efficiency varied on the position of the delivery channel with respect to the two recapture channels. In a symmetrical position where the delivery channel was set in between the two recapture channels (Figure 3f, SI Figure 7), one in approximately four molecules (24.5%) underwent transfer and stalling. This fraction decreased to 14.5 % when the delivery channel was in an asymmetric position compared to the recapture channels. The latter can be attributed to the different electrophoretic forces experienced by the DNA in both cases. The probability of simultaneously threading and thus stalling a molecule is higher when the two recapture pores exert a force equal in magnitude on the molecule leaving the delivery channel. This case only happens in the symmetric arrangement where the delivery channel is equally distant from the recapture channels (given the same voltage applied). In contrast, in the asymmetric configuration, the DNA transport is mainly dominated by the pore located closer to the delivery channel, leaving little or no space for the second recapture pore to interact with the DNA molecule exiting the delivery channel. Notably, in both the symmetric and the asymmetric scenario, pore-to-pore transfer remained the preferred route for the DNA molecules (68 % and 80 % of cases for symmetric and asymmetric bias configuration respectively Figure 3f).

The quad-barrel nanopore can also be re-configured for operation in a very efficient competition mode where all channels are held at the same positive potentials. In this case, DNA molecules were initially driven towards the tip of the nanopipette, where they experienced the electrophoretic force of 4 nanopores. As a result of this molecular tug-of-war, 15% - 20% of coincident events were observed per channel. For instance, around 10 % of dual pore events recorded between adjacent pores (Ch_1-Ch_2 ≈11.5%, Ch_2-Ch_3 ≈ 6.3%, Ch_3-Ch_4 ≈ 7.4%, Ch_4-Ch_1 ≈ 8.5 %) and less than 1% for opposite nanopores (Ch_1-Ch_3 ≈0.7%, Ch_2-Ch_4 ≈1.3%), SI Figure 8. This percentage is a function of the number of competing channels (e.g., 2 or 3), as can be seen in SI Figure 9. Approximately 1% of the overall events were coincident in either three or four channels. In this case, likely, different segments of the same DNA molecule were momentarily threaded in different nanopores. Intuitively, the larger the molecule and its radius of gyration, the more likely it is to interact with multiple pores.

A significant advantage of using a quad-barrel nanopore is that each of the four channels can be independently addressed; however, this device can also be operated using a simpler electronic setup. Achieving single-molecule optical and electrical detection of λ-DNA was made possible by using a single head-stage amplifier (SI Figure 10). The four working electrodes were connected to the same patch-clamp electrode; therefore, the measured ionic current is the sum of the individual ion flux flowing through each nanopore. The potential applied in each channel plays a major role in establishing cooperative detection mechanisms between adjacent nanopores, as well as the type of electrolyte and its ionic strength. For instance, the electro-osmotic flow, resulting from the flow of counter-ions inside and outside each channel, is fundamental in regulating the nanoscale transport between nanopores. High EOF hinders molecules from threading in or outside the pore. Although pore functionalization or the use of polyethylene glycol (PEG) can modulate EOF[38], operating at moderately high salt concentrations (e.g., 1 M or 2 M) where the electric double layer is less than one nanometre appears to be a simple yet robust strategy to reduce the EOF. Notably, the type of electrolyte and ionic strength define the output current signature (thus shape, enhancement, depletion, biphasic, exponential tails, etc.) resulting from the threading of biomolecule as well as affecting its duration and diffusion in the

other channel. We build upon molecular ping-pong type of experiments[39,40] to extend our understanding of DNA diffusion dynamics in a nanopore. We showed that 20 kbp DNA molecules immersed in a 2 M LiCl solution could be captured inside a single channel, and by simply reversing the potential more than 95% were recaptured and threaded back into the bath (Figure 4).

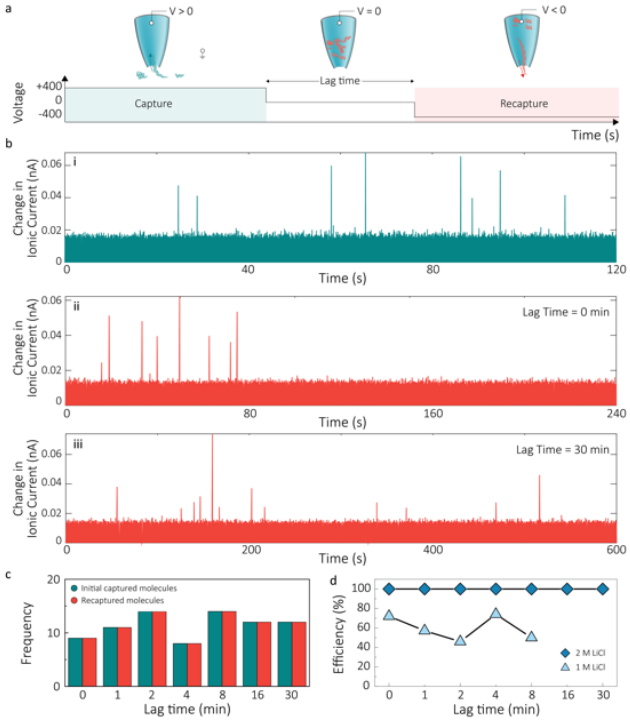

Figure 4. Molecular ping-pong. (a) Schematic showing the setup and procedure for capturing and recapturing DNA. Initially, a positive bias is applied to a single channel and DNA molecules are threaded from the bath to the pipette. This process is halted by setting the potential to zero for a specific amount of time which we define as lag-time. During this time, molecules are free to diffuse inside the barrel, further away from the tip. Finally, the potential is reversed; thus, a negative voltage is applied, and previously captured molecules are recaptured and ejected from the barrel to the bath. (b) Showing ionic current recording of 20 pM 20 kbp DNA in 2 M LiCl, being captured inside the pipette (i) and ejected after a lag-time of 0 (ii) and 30 minutes (iii) respectively. (c) Showing the number of molecules delivered and recaptured and the respective efficiency d) at different lag times.

As shown in Figure 4a, a positive bias (400 mV) was applied for 120 s followed by the potential being switched to 0 for a certain amount of time, which we define as the lag-time. The voltage was then reversed to -400 mV, and translocations were counted. During the lag-time, molecules were expected to diffuse away from the pore. This was confirmed by the lower capture rate and by a lower time after which 50% of the molecules were recaptured ($T_{50\%}$ recapture). $T_{50\%}$ was measured to be approximately 50 s and 170 s for t-lag of 0 and 30 min, respectively (Figure 4b,c). Intuitively, longer lag times enable molecules to travel further away from the tip; however, it was observed that at 2 M LiCl, the recapture efficiency was still 100% even after a lag time of 30 minutes. By halving the salt concentration (e.g., 1 M LiCl), the recapture efficiency dropped to 60 - 70 % (Figure 4d,e). This was explained by considering differences in viscosity[41] which in turn affects the DNA diffusivity. Additionally, the conical pipette geometry can contribute to a more efficient recapture process[42] as molecules propagate over a narrow-angle (3 - 20 deg) along the nanopipette major axis. This is in contrast with solid-state nanopore fabricated in 2D membranes where molecules are freer to diffuse, due to a larger angle outside the sensing region (180 deg). Similarly, high recapture efficiencies (up to 95%) were measured using single barrel nanopipettes indicating that geometry little to no influence (SI Figure 11).

In contrast with what can be considered as a “static approach” (constant DC voltage applied across all channels), in a dynamic approach, voltages were rapidly changed during the experiment, enabling

the possibility to interrogate and detect the same molecule multiple times within distinct nanopores. As shown in Figure 5a, a 20 kbp DNA molecule immersed in a 2 M LiCl bath was captured, detected, and moved subsequently across all four nanopores within less than 4 seconds. In this case, controlling the dynamics of individual molecules was achieved by using an automated protocol which operates channels in pairs: one channel was held at negative potential whereas a second channel was held at a positive potential. Notably, of the four nanopore channels, two of them were temporarily inactive, held at 0 V to avoid any competition during the molecular delivery. In particular, the pair of working channels was quickly switched by reprogramming the bias applied to the device in such a way that a specific DNA molecule was efficiently ejected from one barrel and transferred to the adjacent one. This was also achieved at a different salt concentration of 1 M LiCl (SI Figure 12). A similar approach was used to move and sense one or two molecules across multiple channels of up to 22 times consecutively (SI Figure 13-14). This result confirms that lag-time (elapsed time between the molecule being captured and its subsequent recapture and transfer) is not important in this experimental condition, and the recapture efficiency is approximately ~100 %. Besides, even in this dynamic mode, it was possible to perform more complex operations on the DNA, such as sensing and stretching it across the two pores (Figure 5b).

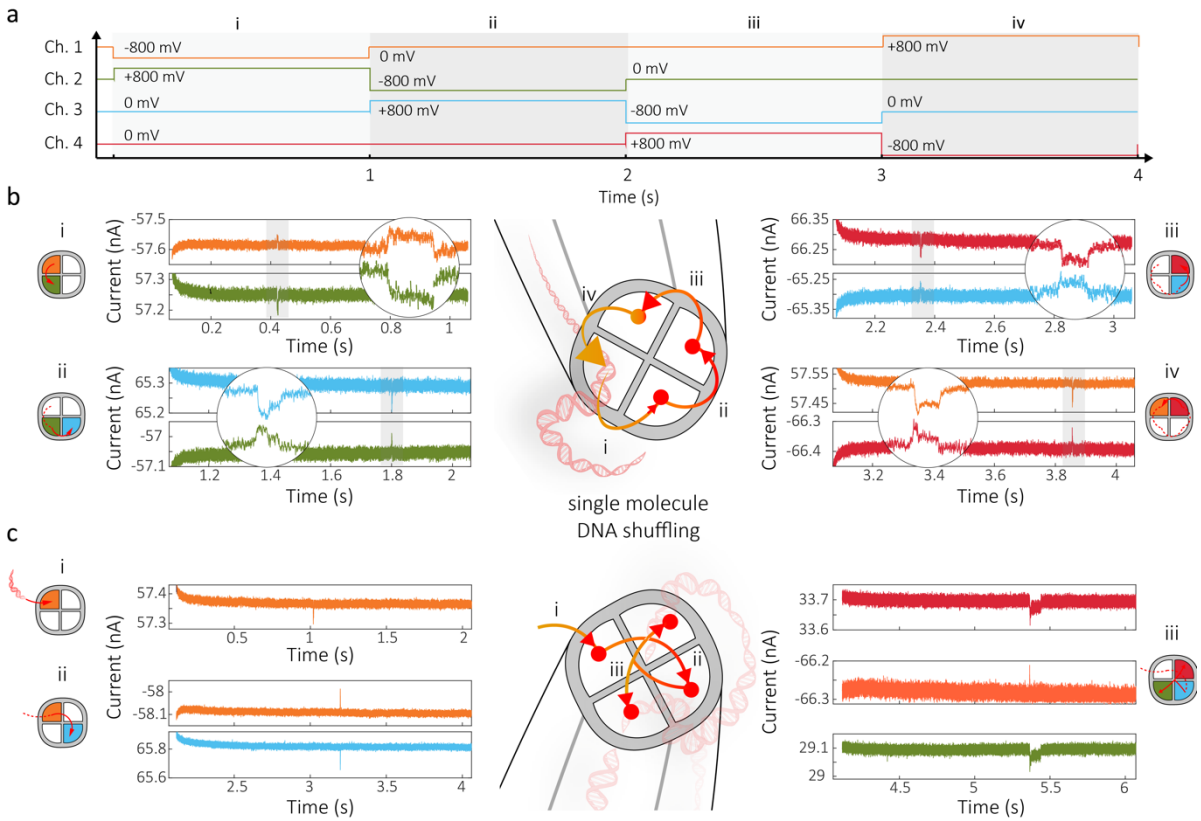

Figure 5. Single molecules sensing and manipulation achieved by dynamically reprogramming the voltage applied to each barrel. (a) A 20 kbp DNA molecule in 2 M LiCl is shuffled across the 4 nanopores. Channels operate in pairs: one delivery channel held at negative potential and one transfer channel held at a positive potential and the working pair changes every second in such a way that, a DNA molecule is continuously ejected from one barrel and transferred to the adjacent one (i, ii, iii, iv). (b) In this sequence, a DNA molecule in 2 M LiCl is first injected in the first barrel (i), transferred to the opposite barrel by reversing the potential (ii) and finally clamped across the other 2 remaining channels as highlighted by the prolonged dwell time (iii).

In conclusion, we presented a reconfigurable multi-nanopore architecture for the detection and manipulation of biomolecules. We demonstrated that the high reproducibility and stability of the fabrication process, which is comparable to single and dual-barrel nanopipettes, makes this quad barrel architecture suitable for single-molecule sensing. It is possible to easily reconfigure this device by individually modulating the electric field across each nanopore, and this gives rise to several unique

cooperative detection modes to move sense and trap DNA molecules as shown in a triple-barrel configuration which combined the advantages of two dual-barrel configurations for enhancing transfer efficiency and temporal resolution of the detected DNA molecules. Notably, this system increases the degrees of freedom in manipulating the dynamics of DNA molecules when operating in dynamic conditions. We envision that this quad-barrel device could be employed for several applications including in the screening field where single-molecule DNA-aptamers vectors are routinely used to detect the presence of specific biomarkers.[43] Quad-nanopores might be used to improve the accuracy in determining the presence and position of this protein along the vector length by re-reading multiple times.

Funding

JBE has been funded in part by an ERC starting (NanoP), proof of concept (NanoPP), and consolidator (NanoPD) grants. AI and JBE acknowledge support from EPSRC grant EP/P011985/1.

Supporting Information

The accompanying supporting information detail the following; SEM images of the nanopores, experimental data on transfer and completion modes, control experiments. This material is available free of charge via the Internet at http://pubs.acs.org.

References

(1) Singh, D.; Wang, Y.; Mallon, J.; Yang, O.; Fei, J.; Poddar, A.; Ceylan, D.; Bailey, S.; Ha, T. Mechanisms of Improved Specificity of Engineered Cas9s Revealed by Single-Molecule FRET Analysis. *Nat. Struct. Mol. Biol.* 2018, *25* (4), 347–354.

(2) Shi, W.; Friedman, A. K.; Baker, L. A. Nanopore Sensing. *Anal. Chem.* 2017, *89* (1), 157–188.

(3) Miles, B. N.; Ivanov, A. P.; Wilson, K. a; Doğan, F.; Japrung, D.; Edel, J. B. Single Molecule Sensing with Solid-State Nanopores: Novel Materials, Methods, and Applications. *Chem. Soc. Rev.* 2013, *42* (1), 15–28.

(4) Carson, S.; Wanunu, M. Challenges in DNA Motion Control and Sequence Readout Using Nanopore Devices. *Nanotechnology* 2015, *26* (7), 1–14.

(5) Squires, A. H.; Hersey, J. S.; Grinstaff, M. W.; Meller, A. A Nanopore-Nanofiber Mesh Biosensor to Control DNA Translocation. *J. Am. Chem. Soc.* 2013, *135* (44), 16304–16307.

(6) Yu, R.-J.; Ying, Y.-L.; Gao, R.; Long, Y.-T. Confined Nanopipette Sensing: From Single Molecules, Single Nanoparticles, to Single Cells. *Angew. Chemie Int. Ed.* 2019, *58* (12), 3706–3714.

(7) Arjmandi-Tash, H.; Belyaeva, L. A.; Schneider, G. F. Single Molecule Detection with Graphene and Other Two-Dimensional Materials: Nanopores and Beyond. *Chem. Soc. Rev.* 2016, *45* (3), 476–493.

(8) Mirsaidov, U.; Comer, J.; Dimitrov, V.; Aksimentiev, A.; Timp, G. Slowing the Translocation of Double-Stranded DNA Using a Nanopore Smaller than the Double Helix. *Nanotechnology* 2010, *21* (39), 395501.

(9) Shankla, M.; Aksimentiev, A. Step-Defect Guided Delivery of DNA to a Graphene Nanopore. *Nat. Nanotechnol.* 2019, 14, 858–865.

(10) Feng, J.; Liu, K.; Bulushev, R. D.; Khlybov, S.; Dumcenco, D.; Kis, A.; Radenovic, A. Identification of Single Nucleotides in MoS2 Nanopores. *Nat. Nanotechnol.* 2015, *10* (12), 1070–1076.

(11) Al Sulaiman, D.; Cadinu, P.; Ivanov, A. P.; Edel, J. B.; Ladame, S. Chemically Modified Hydrogel-

Filled Nanopores: A Tunable Platform for Single-Molecule Sensing. *Nano Lett.* 2018, *18* (9), 6084–6093.

(12) Laucirica, G.; Marmisollé, W. A.; Toimil-Molares, M. E.; Trautmann, C.; Azzaroni, O. Redox-Driven Reversible Gating of Solid-State Nanochannels. *ACS Appl. Mater. Interfaces* 2019, acsami.9b05961.

(13) Lam, M. H.; Briggs, K.; Kastritis, K.; Magill, M.; Madejski, G. R.; McGrath, J. L.; de Haan, H. W.; Tabard-Cossa, V. Entropic Trapping of DNA with a Nanofiltered Nanopore. *ACS Appl. Nano Mater.* 2019, acsanm.9b00606.

(14) Liu, X.; Mihovilovic Skanata, M.; Stein, D. Entropic Cages for Trapping DNA near a Nanopore. *Nat. Commun.* 2015, *6*, 6222.

(15) Belkin, M.; Chao, S.-H.; Jonsson, M. P.; Dekker, C.; Aksimentiev, A. Plasmonic Nanopores for Trapping, Controlling Displacement, and Sequencing of DNA. *ACS Nano* 2015, *9* (11), 10598–10611.

(16) Liu, Y.; Yobas, L. Slowing DNA Translocation in a Nanofluidic Field-Effect Transistor. *ACS Nano* 2016, *10* (4), 3985–3994.

(17) Ren, R.; Zhang, Y.; Nadappuram, B. P.; Akpinar, B.; Klenerman, D.; Ivanov, A. P.; Edel, J. B.; Korchev, Y. Nanopore Extended Field-Effect Transistor for Selective Single-Molecule Biosensing. *Nat. Commun.* 2017, *8* (1), 586.

(18) Xue, L.; Cadinu, P.; Paulose Nadappuram, B.; Kang, M.; Ma, Y.; Korchev, Y.; Ivanov, A. P.; Edel, J. B. Gated Single-Molecule Transport in Double-Barreled Nanopores. *ACS Appl. Mater. Interfaces* 2018, *10* (44), 38621–38629.

(19) Kalman, E. B.; Vlassiouk, I.; Siwy, Z. S. Nanofluidic Bipolar Transistors. *Adv. Mater.* 2008, *20* (2), 293–297.

(20) Zhang, Y.; Liu, X.; Zhao, Y.; Yu, J.-K.; Reisner, W.; Dunbar, W. B. Single Molecule DNA Resensing Using a Two-Pore Device. *Small* 2018, *14* (47), 1801890.

(21) Pud, S.; Chao, S.-H.; Belkin, M.; Verschueren, D.; Huijben, T.; van Engelenburg, C.; Dekker, C.; Aksimentiev, A. Mechanical Trapping of DNA in a Double-Nanopore System. *Nano Lett.* 2016, *16* (12), 8021–8028.

(22) Tsutsui, M.; Yokota, K.; Nakada, T.; Arima, A.; Tonomura, W.; Taniguchi, M.; Washio, T.; Kawai, T. Particle Capture in Solid-State Multipores. *ACS Sensors* 2018, *3* (12), 2693–2701.

(23) Duan, L.; Yobas, L. Label-Free Multiplexed Electrical Detection of Cancer Markers on a Microchip Featuring an Integrated Fluidic Diode Nanopore Array. *ACS Nano* 2018, *12* (8), 7892–7900.

(24) Cadinu, P.; Paulose Nadappuram, B.; Lee, D. J.; Sze, J. Y. Y.; Campolo, G.; Zhang, Y.; Shevchuk, A.; Ladame, S.; Albrecht, T.; Korchev, Y.; et al. Single Molecule Trapping and Sensing Using Dual Nanopores Separated by a Zeptoliter Nanobridge. *Nano Lett.* 2017, *17* (10), 6376–6384.

(25) Liu, X.; Zhang, Y.; Nagel, R.; Reisner, W.; Dunbar, W. B. Controlling DNA Tug-of-War in a Dual Nanopore Device. 2018, 1–33.

(26) Liu, X.; Zimny, P.; Zhang, Y.; Rana, A.; Nagel, R.; Reisner, W.; Dunbar, W. B. Flossing DNA in a Dual Nanopore Device. *Small* 2020, *16* (3), 1905379.

(27) Pud, S.; Chao, S.-H.; Belkin, M.; Verschueren, D.; Huijben, T.; van Engelenburg, C.; Dekker, C.; Aksimentiev, A. Mechanical Trapping of DNA in a Double-Nanopore System. *Nano Lett.* 2016,

16 (12), 8021–8028.

(28) Pedone, D.; Langecker, M.; Abstreiter, G.; Rant, U. A Pore-Cavity-Pore Device to Trap and Investigate Single Nanoparticles and DNA Molecules in a Femtoliter Compartment: Confined Diffusion and Narrow Escape. *Nano Lett.* 2011, *11* (4), 1561–1567.

(29) Harms, Z. D.; Mogensen, K. B.; Nunes, P. S.; Zhou, K.; Hildenbrand, B. W.; Mitra, I.; Tan, Z.; Zlotnick, A.; Kutter, J. P.; Jacobson, S. C. Nanofluidic Devices with Two Pores in Series for Resistive-Pulse Sensing of Single Virus Capsids. *Anal. Chem.* 2011, *83* (24), 9573–9578.

(30) Cadinu, P.; Campolo, G.; Pud, S.; Yang, W.; Edel, J. B.; Dekker, C.; Ivanov, A. P. Double Barrel Nanopores as a New Tool for Controlling Single-Molecule Transport. *Nano Lett.* 2018, *18* (4), 2738–2745.

(31) Rodolfa, K. T.; Bruckbauer, A.; Zhou, D.; Schevchuk, A. I.; Korchev, Y. E.; Klenerman, D. Nanoscale Pipetting for Controlled Chemistry in Small Arrayed Water Droplets Using a Double-Barrel Pipet. *Nano Lett.* 2006, *6* (2), 252–257.

(32) Perry, D.; Momotenko, D.; Lazenby, R. A.; Kang, M.; Unwin, P. R. Characterization of Nanopipettes. *Anal. Chem.* 2016, *88* (10), 5523–5530.

(33) Nadappuram, B. P.; McKelvey, K.; Al Botros, R.; Colburn, A. W.; Unwin, P. R. Fabrication and Characterization of Dual Function Nanoscale PH-Scanning Ion Conductance Microscopy (SICM) Probes for High Resolution PH Mapping. *Anal. Chem.* 2013, *85* (17), 8070–8074.

(34) Nadappuram, P. B.; McKelvey, K.; Byers, J. C.; Güell, A. G.; Colburn, A. W.; Lazenby, R. A.; Unwin, P. R. Quad-Barrel Multifunctional Electrochemical and Ion Conductance Probe for Voltammetric Analysis and Imaging. *Anal. Chem.* 2015, *87* (7), 3566–3573.

(35) Schoch, R. B.; Han, J.; Renaud, P. Transport Phenomena in Nanofluidics. *Rev. Mod. Phys.* 2008, *80* (3), 839–883.

(36) Wei, C.; Bard, A. J.; Feldberg, S. W. Current Rectification at Quartz Nanopipet Electrodes. *Anal. Chem.* 1997, *69* (22), 4627–4633.

(37) Chen, K.; Bell, N. A. W.; Kong, J.; Tian, Y.; Keyser, U. F. Direction- and Salt-Dependent Ionic Current Signatures for DNA Sensing with Asymmetric Nanopores. *Biophys. J.* 2017, *112* (4), 674–682.

(38) Ermann, N.; Hanikel, N.; Wang, V.; Chen, K.; Weckman, N. E.; Keyser, U. F. Promoting Single-File DNA Translocations through Nanopores Using Electro-Osmotic Flow. *J. Chem. Phys.* 2018, *149* (16), 163311.

(39) Gershow, M.; Golovchenko, J. A. Recapturing and Trapping Single Molecules with a Solid-State Nanopore. *Nat. Nanotechnol.* 2007, *2* (12), 775–779.

(40) Plesa, C.; Cornelissen, L.; Tuijtel, M. W.; Dekker, C. Non-Equilibrium Folding of Individual DNA Molecules Recaptured up to 1000 Times in a Solid State Nanopore. *Nanotechnology* 2013, *24* (47), 475101.

(41) Tanaka, K.; Tamamushi, R. A Physico-Chemical Study of Concentrated Aqueous Solutions of Lithium Chloride. *Zeitschrift für Naturforsch. A* 1991, *46* (1–2), 141–147.

(42) Bell, N. A. W.; Chen, K.; Ghosal, S.; Ricci, M.; Keyser, U. F. Asymmetric Dynamics of DNA Entering and Exiting a Strongly Confining Nanopore. *Nat. Commun.* 2017, *8* (1), 1–8.

(43) Sze, J. Y. Y.; Ivanov, A. P.; Cass, A. E. G.; Edel, J. B. Single Molecule Multiplexed Nanopore Protein Screening in Human Serum Using Aptamer Modified DNA Carriers. *Nat. Commun.*

2017, *8* (1), 1552.

TOC Image